

# Effects of –OH Groups on Fe<sub>3</sub>O<sub>4</sub> Particles on the Heterogeneous Coating in a Hydrous Alumina Coating Process

Hai-Xia Wu, Ting-Jie Wang,\* and Yong Jin

Department of Chemical Engineering, Tsinghua University, Beijing 100084, China

The effects of the –OH groups on Fe<sub>3</sub>O<sub>4</sub> particles on heterogeneous coating in an aqueous process were studied. Three kinds of Fe<sub>3</sub>O<sub>4</sub> particles, nontreated, base-treated, and microwave hydrothermally treated, with different amounts and nature of –OH groups on their surfaces were used in a hydrous alumina coating process. The –OH groups on the Fe<sub>3</sub>O<sub>4</sub> particles were characterized by TGA, FTIR, and base titration. The relative amounts of –OH groups were in the order microwave hydrothermally treated > nontreated > base treated. The microwave hydrothermally treated Fe<sub>3</sub>O<sub>4</sub> particles were basic at pH <7.7 and acidic at pH >7.7, while the nontreated and base-treated particles did not show clear acidic or basic nature. HRTEM images showed that the microwave hydrothermally treated Fe<sub>3</sub>O<sub>4</sub> particles were more easily film coated by hydrous alumina, while the nontreated and base-treated Fe<sub>3</sub>O<sub>4</sub> particles gave rise to more homogeneous precipitation of hydrous alumina under the same condition. It is inferred that the precipitation and reaction occurred at surface hydroxyl sites in the coating process.

## 1. Introduction

During a particle coating process, the homogeneous nucleation that often occurs in an aqueous precipitation process, e.g., in ultrafine particle coating and supported catalyst preparation,<sup>1–3</sup> greatly reduces the coating quality and should be avoided. It is necessary to determine the key factor and control it to promote heterogeneous coating on the core particle surface, and to limit the homogeneous nucleation in the bulk.

Heterogeneous coating is usually controlled by adjusting the concentration of the solution complex through changing the coating conditions, e.g., concentration of coating reagent, pH, and temperature.<sup>4</sup> When the concentration of the solution complex exceeds critical supersaturation for heterogeneous precipitation, heterogeneous coating on the core particles occurs. When the concentration of the solution complex exceeds critical supersaturation for homogeneous nucleation, bulk precipitation and homogeneous nucleation occur in the liquid, and this prevents good coating. Thus, the addition of the hydroxide ions in the whole solution needs to be uniformly and carefully controlled to avoid local supersaturation and homogeneous precipitation in the bulk.<sup>5</sup> Therefore, the supersaturation of the solution complex is one of the key factors in heterogeneous coating.

Merikhi et al.<sup>6</sup> reported that condensation and interaction occurred between the solution complex Si–OH and the –OH groups on the core particle surface in the process of SiO<sub>2</sub> coating on ZnS particle surface. When the ZnS particles were treated by different methods, namely, washing with H<sub>2</sub>O, HCl, and H<sub>2</sub>O<sub>2</sub> and precoated with ZnO colloids, the SiO<sub>2</sub> coating results were different. This showed that the surface properties of the core particles affect the heterogeneous coating process. Wu et al.<sup>7</sup> also reported this phenomenon, and interpreted the process of the nucleation and growth of coating onto the core particle surface through a condensation between OH–Al species precursors and –OH groups on the TiO<sub>2</sub> particle surface. Barrere et al.<sup>8</sup> reported that the heterogeneous nucleation and growth of Ca–P is initiated by chemical bonding of nanosized clusters

with –OH groups on titanium surface forming an interfacial unstructured matrix. Burattin et al.<sup>3</sup> explained that the precipitation depended on a kinetic competition between the reaction of precursor condensation and precursor reaction on the core particle surface.

It is known that there exist a number of –OH groups on oxide particle surfaces.<sup>9</sup> Many methods were proposed to measure the hydroxyl densities on oxides, such as reaction with Grignard reagents, surface acid–base titration, dehydration by heating, IR spectroscopy, tritium exchange with hydroxyl protons, and crystallographic calculations.<sup>10–13</sup> The acid–base interaction/condensation that occurs on oxide surfaces depends on the nature of the –OH groups on the oxide surfaces.<sup>14</sup>

In this paper, the effects of the –OH groups of the core particle surface on heterogeneous coating and homogeneous nucleation were investigated. The amount and nature of the –OH groups on Fe<sub>3</sub>O<sub>4</sub> particles that were nontreated, base-treated, and microwave hydrothermally treated were examined by thermogravimetric analysis (TGA), Fourier transform infrared (FTIR) spectroscopy, and surface base titration. The coating morphologies were compared for the differently treated particles.

## 2. Experimental Section

**2.1. Reagents.** The Fe<sub>3</sub>O<sub>4</sub> particles used were of cubic shape, were 400 nm in mean diameter, were nonporous, and had a surface area of 4.53 m<sup>2</sup>/g (Commercial Iron Black, Tianjin Copy Technology Institute, China). The commercial TiO<sub>2</sub> particles used were from the sulfate process, were of rutile structure, were 200 nm in mean diameter, were nonporous, and had a surface area of 6.54 m<sup>2</sup>/g (Commercial Titania, Zhengjiang Titania Co., Ltd., China). Other chemicals used in the experiments were analytical reagents of AR grade. The particle size and surface area were measured in this research.

**2.2. Treatment of the Fe<sub>3</sub>O<sub>4</sub> Particles. 2.2.1. Base Treatment.** A 5 g sample of Fe<sub>3</sub>O<sub>4</sub> particles was dispersed in 100 mL of NaOH solution (1.0 mol/L) by ultrasonic treatment for 20 min (80 W, Shanghai KuDos Ultrasonic Instrument Co., Ltd., China). The base treatment of the Fe<sub>3</sub>O<sub>4</sub> particles in a NaOH solution was performed for 8 h. The particles were then washed repeatedly by deionized water until the filtrate was neutral. The

\* To whom correspondence should be addressed. Tel.: +86-10-62788993. Fax: +86-10-62772051. E-mail: wangtj@mail.tsinghua.edu.cn.

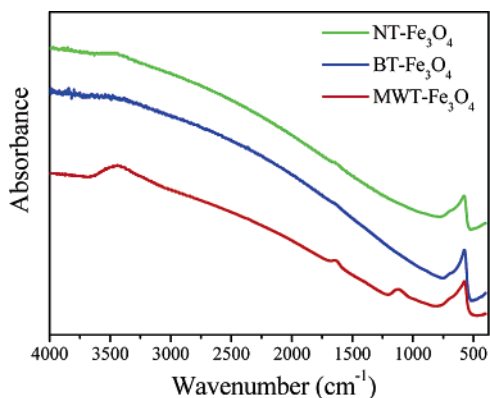


Figure 1. FTIR spectra of NT-Fe<sub>3</sub>O<sub>4</sub>, BT-Fe<sub>3</sub>O<sub>4</sub>, and MWT-Fe<sub>3</sub>O<sub>4</sub> particles.

Fe<sub>3</sub>O<sub>4</sub> particle cake was dried at 60 °C under vacuum for 20 h and crushed into dispersed particles. Then, the base-treated Fe<sub>3</sub>O<sub>4</sub> particles were ready for further characterization or coating.

**2.2.2. Microwave Hydrothermal Treatment.** A 5 g sample of Fe<sub>3</sub>O<sub>4</sub> particles was dispersed in 100 mL of deionized water by ultrasonic treatment for 20 min. The suspension was put into a microwave oven and treated at 2450 MHz for 5 min. The Fe<sub>3</sub>O<sub>4</sub> particles were filtered and dried at 60 °C under vacuum for 20 h, and crushed into dispersed particles. Then, the microwave hydrothermally treated Fe<sub>3</sub>O<sub>4</sub> particles were ready for further characterization or coating.

**2.3. Base Titration of the Fe<sub>3</sub>O<sub>4</sub> Particle Suspension.** Base titrations were carried out in a flask equipped with a pH meter and peristaltic pump as described previously.<sup>11</sup> All titrations were carried out at 20 °C under N<sub>2</sub> protection to avoid the influence of CO<sub>2</sub> dissolution into the suspension.

A blank experiment was carried out by titrating a NaOH solution (0.010 mol/L) with a mixture of 5 mL of oxalic acid solution (0.010 mol/L) and 70 mL of deionized water to pH 10. The base titrations for the Fe<sub>3</sub>O<sub>4</sub> particles were performed as follow: (1) 50 mg of Fe<sub>3</sub>O<sub>4</sub> particles was dispersed into 70 mL of deionized water to form a suspension; (2) 5 mL of oxalic acid solution (0.010 mol/L) was uniformly mixed into the suspension; (3) NaOH solution (0.010 mol/L) was titrated into the suspension until pH 10.

**2.4. Coating Process.** The experiments were carried out in a flask with the temperature and pH measured online with a thermometer and pH meter, respectively, as in our previous research.<sup>15</sup> The temperature was controlled by a constant-temperature bath. The core particles, at a concentration of 50 g/L, were dispersed in deionized water by continuous ultrasonic treatment for 30 min before the coating. Then, Al<sub>2</sub>(SO<sub>4</sub>)<sub>3</sub> solution (0.3 mol/L) and NaOH solution (1 mol/L) were titrated into the particle suspension simultaneously. The particle suspension was stirred strongly and adjusted to a set pH by controlling the titrating speed of the NaOH solution, while the titrating speed of the Al<sub>2</sub>(SO<sub>4</sub>)<sub>3</sub> solution was kept constant. After titration, the suspension was aged for 2 h with stirring. Then, the coated particles were filtered and washed repeatedly until SO<sub>4</sub><sup>2-</sup> was no longer detected using a BaCl<sub>2</sub> solution. This was followed by drying for 12 h at 120 °C.

**2.5. Measurements and Characterization.** **2.5.1. -OH Group Measurements.** A Fourier transform IR spectrometer (NICOLET 5DX, USA) was used for IR absorption spectroscopy. Thermogravimetric analysis (TGA2050, TA Instruments, USA) was used to determine the quantity of the -OH groups on the particle surface. An automated surface and pore size

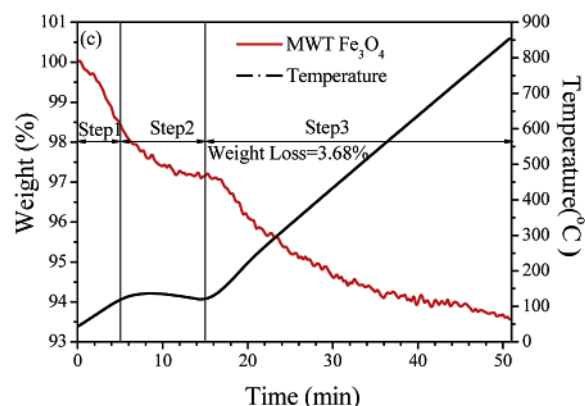
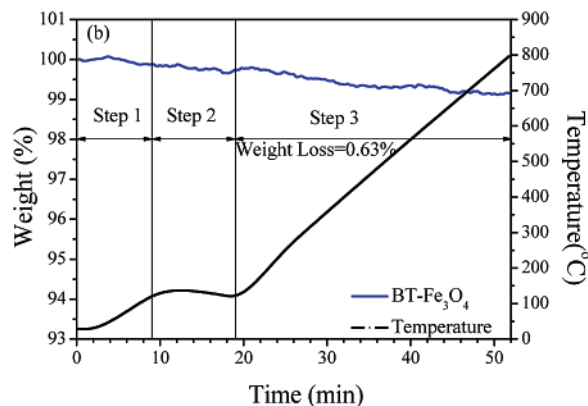
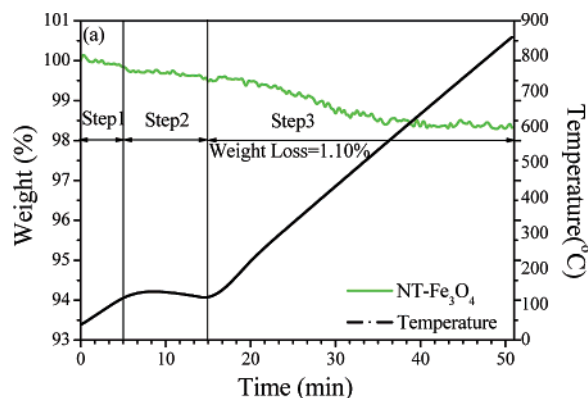


Figure 2. TGA curves of Fe<sub>3</sub>O<sub>4</sub> particles. (a) NT-Fe<sub>3</sub>O<sub>4</sub>; (b) BT-Fe<sub>3</sub>O<sub>4</sub>; (c) MWT-Fe<sub>3</sub>O<sub>4</sub>.

analyzer (Autosorb-1-C, Quantachrome, USA) was used for particle surface area analysis.

**2.5.2. Surface Characterization.** The morphology and structure of the hydrous alumina coating on the particle surface were examined by high-resolution transmission electron microscopy (HRTEM; JEM-2011, JEOL Co., Japan). The chemical binding energy of the atoms on the particle surface was determined by X-ray photoelectron spectroscopy (XPS; PHI-5300, Perkin-Elmer, Eden Prairie, MN).

**2.5.3. Particle Size Measurement.** The particle size was measured by a particle sizer (ZetaPALS, Brookhaven Instruments, USA) with a measurement range of 2 nm–3 μm.

### 3. Results and Discussion

The surface oxygen of oxides exposed to a moist environment or aqueous solution reacts with water, forming -OH groups on the particle surface.<sup>10</sup> The -OH groups on the particle surface accept or provide different amounts of protons at different

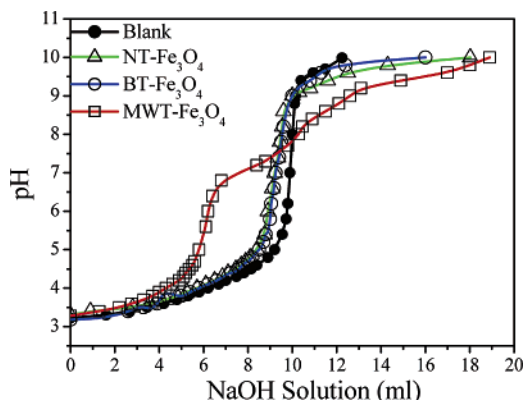


**Figure 3.** NaOH titration curves of NT-Fe<sub>3</sub>O<sub>4</sub>, BT-Fe<sub>3</sub>O<sub>4</sub>, and MWT-Fe<sub>3</sub>O<sub>4</sub> suspensions and the blank solution.

pHs.<sup>16,17</sup> They are acidic when they provide or exchange protons with the ions in the solution and basic when they accept protons. The amount and nature of the  $-OH$  groups play an important role in surface reaction processes.

**3.1.  $-OH$  Groups on Fe<sub>3</sub>O<sub>4</sub> Particles. 3.1.2. FTIR Characterization.** The FTIR spectra of nontreated Fe<sub>3</sub>O<sub>4</sub> (NT-Fe<sub>3</sub>O<sub>4</sub>), base-treated Fe<sub>3</sub>O<sub>4</sub> (BT-Fe<sub>3</sub>O<sub>4</sub>), and microwave hydrothermally treated Fe<sub>3</sub>O<sub>4</sub> (MWT-Fe<sub>3</sub>O<sub>4</sub>) are shown in Figure 1. It is seen that all the spectra show a strong peak at  $573\text{ cm}^{-1}$ , which coincides with the standard spectrum of Fe<sub>3</sub>O<sub>4</sub>.<sup>18</sup>

For NT-Fe<sub>3</sub>O<sub>4</sub>, the spectrum band of  $-OH$  groups and adsorbed water on the particle surface in the range of  $3000\text{--}3500\text{ cm}^{-1}$  was very weak. For BT-Fe<sub>3</sub>O<sub>4</sub>, which was treated for 8 h and followed by vacuum desiccation, the spectrum band of  $-OH$  groups and adsorbed water on the particle surface in the range of  $3000\text{--}3500\text{ cm}^{-1}$  could hardly be seen. This is because the  $-OH$  groups on BT-Fe<sub>3</sub>O<sub>4</sub> were removed by the long-time base treatment. However, for MWT-Fe<sub>3</sub>O<sub>4</sub>, the spectrum band of surface  $-OH$  groups and adsorbed water on the particle surface in the range of  $3000\text{--}3500\text{ cm}^{-1}$  was stronger compared with that of NT-Fe<sub>3</sub>O<sub>4</sub> and BT-Fe<sub>3</sub>O<sub>4</sub>. When a dielectric material is put in a microwave field, the dipoles align and flip due to the alternating field. Different materials respond differently in a microwave field.<sup>19</sup> The Fe element in Fe<sub>3</sub>O<sub>4</sub> has a variable valence, and the strong dissipation of microwave energy in the material results in a significant temperature increase, compared to other materials. In exploratory experiments, when a Fe<sub>3</sub>O<sub>4</sub> suspension and TiO<sub>2</sub> suspension of the same concentration and volume in separate beakers without seals were treated in a microwave oven under the same condition, it was found that the Fe<sub>3</sub>O<sub>4</sub> suspension was dried out and the volume of the TiO<sub>2</sub> suspension changed less. Therefore, it is inferred that the temperature of the MWT-Fe<sub>3</sub>O<sub>4</sub> particles is much higher than in the water bulk phase, and adsorbed water on the particle surface was easily dissociated to form  $-OH$  groups.

The band intensities in the range of  $3000\text{--}3500\text{ cm}^{-1}$  were compared using the  $573\text{ cm}^{-1}$  peak as the reference, and the order is as follows:  $I(\text{MWT-Fe}_3\text{O}_4) > I(\text{NT-Fe}_3\text{O}_4) > I(\text{BT-Fe}_3\text{O}_4)$ ; this indicates that the relative amount of  $-OH$  groups on the samples is  $\text{MWT-Fe}_3\text{O}_4 > \text{NT-Fe}_3\text{O}_4 > \text{BT-Fe}_3\text{O}_4$ .

**3.1.2.  $-OH$  Group Measurements.** The  $-OH$  groups on Fe<sub>3</sub>O<sub>4</sub> particle surface were measured using thermogravimetric analysis as described in the literature.<sup>20,21</sup> The weight-loss curves for the three kinds of Fe<sub>3</sub>O<sub>4</sub> particles are shown in Figure 2. A heating rate of  $10\text{ }^\circ\text{C}/\text{min}$  was used in step 1 in Figure 2, kept at  $120\text{ }^\circ\text{C}$  for 10 min in step 2, and then the samples were further heated from  $120$  to  $800\text{ }^\circ\text{C}$  at a heating rate of  $20\text{ }^\circ\text{C}/\text{min}$

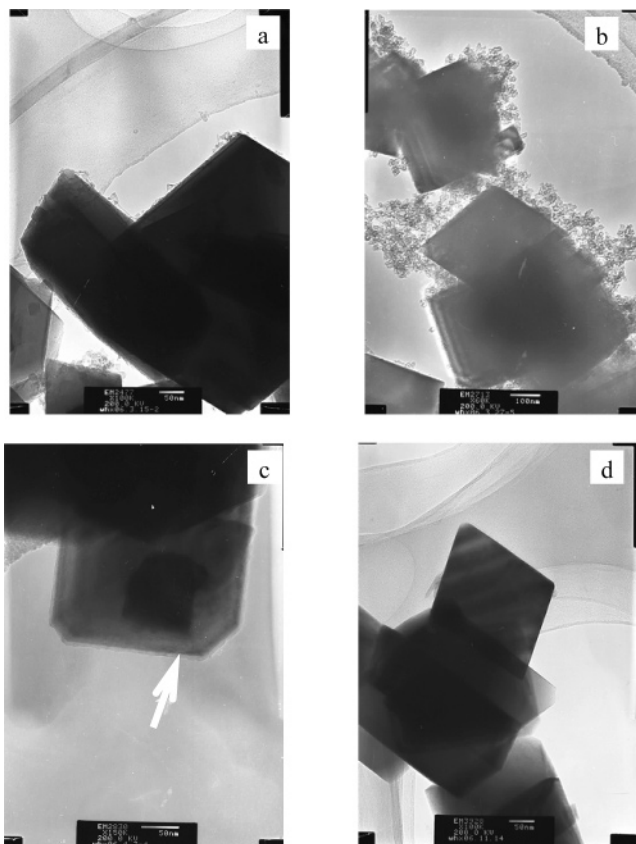


**Figure 4.** HRTEM images of coated Fe<sub>3</sub>O<sub>4</sub> particles (pH 6,  $20\text{ }^\circ\text{C}$ ): (a) NT-Fe<sub>3</sub>O<sub>4</sub>; (b) BT-Fe<sub>3</sub>O<sub>4</sub>; (c) MWT-Fe<sub>3</sub>O<sub>4</sub>; (d) noncoated-Fe<sub>3</sub>O<sub>4</sub>.

step 3. To avoid the influence of oxidation, the samples were kept under N<sub>2</sub> protection during the whole heating process. Adsorbed water was considered to be completely removed after 10 min at  $120\text{ }^\circ\text{C}$ . The  $-OH$  groups on the particle surface can be estimated from the weight loss from  $120$  to  $800\text{ }^\circ\text{C}$ .

From Figure 2, the weight losses from  $120$  to  $800\text{ }^\circ\text{C}$  in step 3 for NT-Fe<sub>3</sub>O<sub>4</sub>, BT-Fe<sub>3</sub>O<sub>4</sub>, and MWT-Fe<sub>3</sub>O<sub>4</sub> particles were calculated to be 1.10%, 0.63%, and 3.68%, respectively. The BET surface areas for NT-Fe<sub>3</sub>O<sub>4</sub>, BT-Fe<sub>3</sub>O<sub>4</sub>, and MWT-Fe<sub>3</sub>O<sub>4</sub> particles were 4.53, 5.00, and 4.65 m<sup>2</sup>/g, respectively. This shows that the surface density of  $-OH$  groups on MWT-Fe<sub>3</sub>O<sub>4</sub> particles is about 3 times that of NT-Fe<sub>3</sub>O<sub>4</sub> particles, and 6 times that of BT-Fe<sub>3</sub>O<sub>4</sub> particles.

**3.2. Acid/Base Properties of  $-OH$  Groups.** The NaOH solution titrations for characterizing the acid/base properties of the  $-OH$  groups on the three kinds of Fe<sub>3</sub>O<sub>4</sub> particle surfaces are shown in Figure 3. Since the Fe<sub>3</sub>O<sub>4</sub> particles were nonporous, equilibration was very quick during titration. The amounts of NaOH solution titrated to reach a set pH 10 for the three kinds of Fe<sub>3</sub>O<sub>4</sub> particles all exceeded the amount needed in the blank solution. All the curves for the three kinds of Fe<sub>3</sub>O<sub>4</sub> particles have a crossing point with the blank curve, which shows that the particles have different acidic and basic properties at different pHs.

The titration curves of the BT-Fe<sub>3</sub>O<sub>4</sub> and NT-Fe<sub>3</sub>O<sub>4</sub> samples almost met with the blank curve at the same point, pH 9. It can be seen from Figure 3 that NT-Fe<sub>3</sub>O<sub>4</sub> and BT-Fe<sub>3</sub>O<sub>4</sub> are basic at pH  $< 9$ , and are acidic at pH  $> 9$ , by comparing with the blank curve. At pH  $< 9$ , the consumption of NaOH solution for NT-Fe<sub>3</sub>O<sub>4</sub> and BT-Fe<sub>3</sub>O<sub>4</sub> were nearly the same. This indicates that the base treatment had little effect on the basic  $-OH$  groups. At pH  $> 9$ , the consumption of NaOH solution for BT-Fe<sub>3</sub>O<sub>4</sub> is less than that for NT-Fe<sub>3</sub>O<sub>4</sub>. This indicates that the base

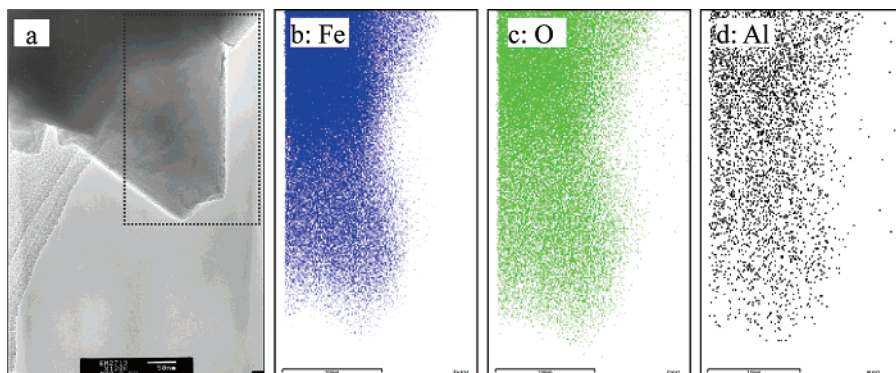


**Figure 5.** HRTEM image and EDS mapping of coated MWT-Fe<sub>3</sub>O<sub>4</sub> particles: (a) HRTEM image; (b) EDS mapping of Fe in selected area of (a); (c) EDS mapping of O in selected area of (a); (d) EDS mapping of Al in selected area of (a).

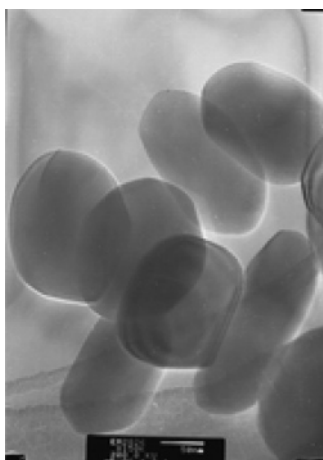


**Figure 6.** HRTEM images of uncoated TiO<sub>2</sub> particles.

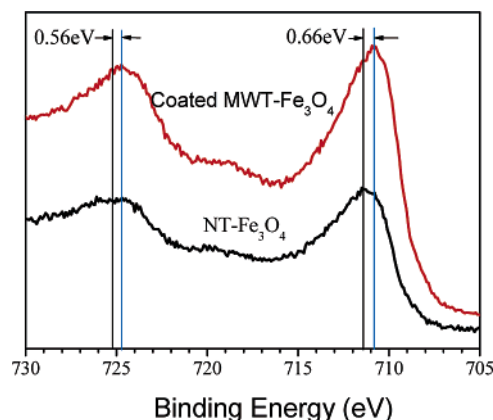


**Figure 8.** XPS spectra of Fe peaks of uncoated and coated MWT-Fe<sub>3</sub>O<sub>4</sub> particles.

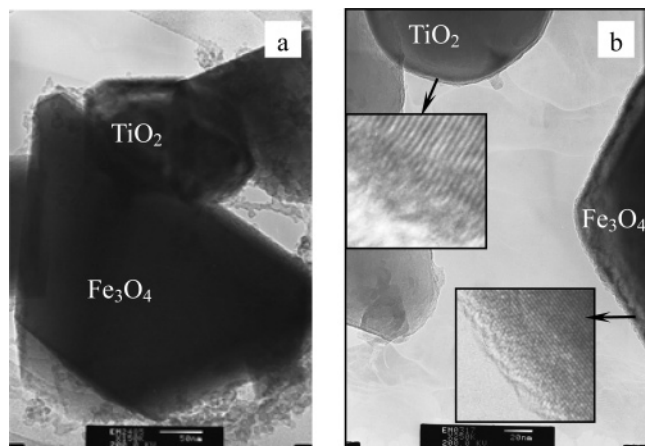


**Figure 7.** HRTEM images of coating morphology of Fe<sub>3</sub>O<sub>4</sub> and TiO<sub>2</sub> particle mixtures: (a) NT-Fe<sub>3</sub>O<sub>4</sub> and TiO<sub>2</sub>; (b) MWT-Fe<sub>3</sub>O<sub>4</sub> and TiO<sub>2</sub>.

treatment had removed some acidic  $-OH$  groups on the Fe<sub>3</sub>O<sub>4</sub> particle surface. The titration curve of MWT-Fe<sub>3</sub>O<sub>4</sub> had a crossing point with the blank curve at pH 7.7. At pH < 7.7, the MWT-Fe<sub>3</sub>O<sub>4</sub> particles consume much less NaOH solution to reach the same pH compared with the blank curve, which indicates that the MWT-Fe<sub>3</sub>O<sub>4</sub> particles are more strongly basic. At pH > 7.7, the MWT-Fe<sub>3</sub>O<sub>4</sub> particles consume much more NaOH solution to reach the same pH compared with the blank curve, which indicates that the MWT-Fe<sub>3</sub>O<sub>4</sub> particles are more strongly acidic.

At a fixed pH, the difference in the amount of titrated NaOH solution between the Fe<sub>3</sub>O<sub>4</sub> samples and the blank reflects the amount of acid or base  $-OH$  groups on the particle surface at

that pH, which also reflects the activity of the  $-OH$  groups. Figure 3 shows that the amounts of acid and base groups on the MWT-Fe<sub>3</sub>O<sub>4</sub> particles are both more than those on the other two particle surfaces at almost all the measured pHs. Thus, the  $-OH$  groups on the MWT-Fe<sub>3</sub>O<sub>4</sub> particle surfaces have a higher reactivity compared with those of NT-Fe<sub>3</sub>O<sub>4</sub> and BT-Fe<sub>3</sub>O<sub>4</sub>.

**3.3. Coatings of Fe<sub>3</sub>O<sub>4</sub> Particles.** The three kinds of particles, NT-Fe<sub>3</sub>O<sub>4</sub>, BT-Fe<sub>3</sub>O<sub>4</sub>, and WMT-Fe<sub>3</sub>O<sub>4</sub>, were coated at the same experimental condition as used in our previous work.<sup>15</sup> The morphologies of the three coated Fe<sub>3</sub>O<sub>4</sub> particles, as well as noncoated Fe<sub>3</sub>O<sub>4</sub> particles, are shown in Figure 4. The Fe<sub>3</sub>O<sub>4</sub> particles can be recognized from their cubic shape.

Although the coating conditions, namely, the temperature, pH value, concentration of the core particles, coating reagent, etc., were all the same, the coating morphologies on the three kinds of particles were different. Figure 4a,b shows the morphology of coated NT-Fe<sub>3</sub>O<sub>4</sub> and BT-Fe<sub>3</sub>O<sub>4</sub> particles. There was almost no film coating on the particle surface, but there were many hydroxide alumina particles around them. Figure 4c shows the morphology of the coated MWT-Fe<sub>3</sub>O<sub>4</sub> particles. It can be seen that there is a layer of continuous film coating on the particle surface.

Figure 5 shows the morphology of the coated MWT-Fe<sub>3</sub>O<sub>4</sub> particles and the corresponding element distribution map from a selected area electron microscope energy-dispersive spectrometer (EDS). The selected particle and selected area are shown in Figure 5a, and the EDS mapping for Fe, O, and Al are shown in Figure 5b, Figure 5c, and Figure 5d, respectively. Figure 5b–d clearly show that the Fe, O, and Al elements were uniformly distributed, indicating that the hydrous alumina was uniformly coated on the particle surface as a film. The weak

intensity in Figure 5d compared with those of Fe and O reflects the thin film coating of Al.

Since the coating conditions for the three kinds of particles were completely the same, and the core particle size, shape, and surface area were almost the same, it can be inferred that it is the amount and character of  $-OH$  groups on the particle surface that promote the forming of the film coating on the MWT- $Fe_3O_4$  particle surface.

**3.4. Coating of a  $Fe_3O_4$  and  $TiO_2$  Mixture.** To identify the effects of the particle surface on the coating process, coating of a  $Fe_3O_4$  and  $TiO_2$  particle mixture was carried out in the same coating environment. The  $TiO_2$  core particles used were ellipsoid-like, as shown in Figure 6. As the  $Fe_3O_4$  particles used were cubic, it is easy to distinguish the  $Fe_3O_4$  and  $TiO_2$  particles by HRTEM inspection, and also the coating morphologies. The coated particle morphology of the mixture is shown in Figure 7. Figure 7a shows the coated NT- $Fe_3O_4$  and  $TiO_2$  particle mixture, and Figure 7b shows the coated MWT- $Fe_3O_4$  and  $TiO_2$  particle mixture. The two mixtures were coated under the same conditions. Figure 7a shows that the cubic NT- $Fe_3O_4$  particles were hardly coated with a film, while the ellipsoid  $TiO_2$  particles were coated with a layer of continuous film. Figure 7b shows that the cubic MWT- $Fe_3O_4$  and ellipsoid  $TiO_2$  particles were both coated with a layer of continuous film. This indicates that the difference in the particle surface  $-OH$  groups between NT- $Fe_3O_4$  and MWT- $Fe_3O_4$  plays a crucial role in heterogeneous coating. The crystal lattices of coated  $TiO_2$  and MWT- $Fe_3O_4$  are shown in Figure 7b.

**3.5. Effect of  $-OH$  Groups.** The XPS spectra of the coated MWT- $Fe_3O_4$  and uncoated NT- $Fe_3O_4$  samples are shown in Figure 8. The two Fe peaks of MWT- $Fe_3O_4$  showed Fe binding energy shifts of  $-0.56$  and  $-0.66$  eV, respectively, compared with that of the uncoated NT- $Fe_3O_4$ . It is inferred that the chemical shifts resulted from the formation of chemical bonds between the coated hydroxide alumina and the MWT- $Fe_3O_4$  particle surface,<sup>22</sup> and the  $-OH$  groups on the particle surface act as reaction sites. There is condensation between the  $-OH$  groups on the particle surface and  $OH-Al$  species, while condensation between  $OH-Al$  species can also occur. The coating process depends on the kinetic competition between the two reactions: the first is the heterogeneous condensation between the  $-OH$  groups on the particle surface and  $OH-Al$  species, which leads to the growth of the coating; the second is the homogeneous condensation among the  $OH-Al$  species, which leads to the formation and the growth of alumina hydroxide particles in the bulk phase.

The surface energy is lower for heterogeneous precipitation than for homogeneous nucleation,<sup>23</sup> so the first reaction is more probable than the latter. However, the heterogeneous precipitation is limited by the density and reactivity of the  $-OH$  groups on the particle surface. When the  $-OH$  groups were removed, e.g., by base treatment, homogeneous nucleation dominated the system and the formation of separated hydroxide alumina particles was preferred. When the amount of  $-OH$  groups was increased, heterogeneous condensation was increased and homogeneous nucleation was limited. Therefore, the particle surface after a microwave hydrothermal treatment is easier to coat with a layer of film.

Therefore,  $-OH$  groups play a key role in the heterogeneous coating process in addition to the supersaturation and solution environment.

#### 4. Conclusions

Experimental results showed that the amount and reactivity of the  $-OH$  groups on the  $Fe_3O_4$  particle surface can be

significantly increased by a microwave hydrothermal treatment and decreased by a base treatment. The  $Fe_3O_4$  particles treated by a microwave hydrothermal treatment can be film coated continuously and uniformly with hydrous alumina. The  $-OH$  groups on the core particle surface play an important role in the coating process, besides the supersaturation and solution environment in the bulk. The  $-OH$  groups act as reaction or condensation sites during the precipitation coating process. A large amount and reactivity of the  $-OH$  groups on the particle surface can speed up heterogeneous coating and limit homogeneous nucleation in the bulk.

#### Acknowledgment

The authors wish to express their appreciation for the financial support of this study by the National Natural Science Foundation of China (NSFC No. 20476051) and the Specialized Research Fund for the Doctoral Program of Higher Education (SRFDP No. 20060003089).

#### Literature Cited

- Alken, B.; Matijevic, E. Preparation and properties of uniform coated inorganic colloidal particles IV. yttrium basic carbonate and yttrium oxide on hematite. *J. Colloid Interface Sci.* **1988**, *126* (2), 645.
- Haq, I.; Matijevic, E. Preparation and properties of uniform coated inorganic colloidal particles. *J. Colloid Interface Sci.* **1997**, *192*, 104.
- Burattin, P.; Che, M.; Louis, C. Molecular approach to the mechanism of deposition-precipitation of the Ni(II) phase on silica. *J. Phys. Chem. B* **1998**, *102*, 2722.
- He, Y. X. Ceramic composites through solution precipitation coating. Ph.D. Dissertation, University of California, Berkeley, CA, 1998.
- Mitchell, T. D.; DeJonghe, L. C. Processing and properties of particulate composites from coated powders. *J. Am. Ceram. Soc.* **1995**, *78* (1), 199.
- Merikhi, J.; Feldmann, C. Adhesion of colloidal  $SiO_2$  particles on ZnS-type phosphor surface. *J. Colloid Interface Sci.* **2000**, *228*, 121.
- Wu, H. X.; Wang, T. J.; Jin, Y. Film coating process of hydrated alumina on  $TiO_2$  particles. *Ind. Eng. Chem. Res.* **2006**, *45*, 1337.
- Barrere, F.; Snelc, M. M. E.; Blitterswijk, C. A. V.; Groot, K. d.; Layrolle, P. Nano-scale study of the nucleation and growth of calcium phosphate coating on titanium implants. *Biomaterials* **2004**, *25*, 2901.
- Chadwick, M. D.; Goodwin, J. W.; Lawson, E. J.; Mills, P. D. A.; Vincent, B. Surface charge properties of colloidal titanium dioxide in ethylene glycol and water. *Colloids Surf., A: Physicochem. Eng. Aspects* **2002**, *203*, 229.
- Tamura, H.; Tanaka, A.; Mita, K.; Furuichi, R. Surface hydroxyl site densities on metal oxides as a measure for the ion-exchange capacity. *J. Colloid Interface Sci.* **1999**, *209*, 225.
- Van der Lee, M. K.; Dillen, A. J.; Bitter, J. H.; De Jong, K. P. Deposition precipitation for the preparation of carbon nanofiber supported Nickel catalysts. *J. Am. Chem. Soc.* **2005**, *127*, 13573.
- Curthoys, G.; Davydov, V. Y.; Kiselev, A. V.; et al. Hydrogen bonding in adsorption on silica. *J. Colloid Interface Sci.* **1974**, *48* (1), 58.
- Ramos, M. A.; Gil, M. H.; Schacht, E. Physical and chemical characterisation of some silicas and silica derivatives. *Powder Technol.* **1998**, *99* (1), 79.
- Erdem, B.; Hunsicker, R. A.; Simmons, G. W.; Sudol, E. D.; Dimonie, V. L.; El-Aasser, M. S. XPS and FTIR surface characterization of  $TiO_2$  particles used in polymer encapsulation. *Langmuir* **2001**, *17*, 2664.
- Wu, H. X.; Wang, T. J.; Jin, Y. Morphology "phase diagram" of the hydrous alumina coating on  $TiO_2$  particles during aqueous precipitation. *Ind. Eng. Chem. Res.* **2006**, *45*, 5274.
- Mullet, M.; Fievet, P.; Reggiani, J. C.; Pagetti, J. Surface electrochemical properties of mixed oxide ceramic membranes: zeta-potential and surface charge density. *J. Membr. Sci.* **1997**, *123*, 255.
- Chadwick, M. D.; Goodwin, J. W.; Lawson, E. J.; Mills, P. D. A.; Vincent, B. Surface charge properties of colloidal titanium dioxide in ethylene glycol and water. *Colloids Surf., A: Physicochem. Eng. Aspects* **2002**, *203*, 229.
- Nyquist, R. A.; Kagel, R. O. *Infrared spectra of inorganic compounds*; Academic Press: New York and London, 1971.

- (19) Tyagi, B.; Chudasama, C. D.; Jasra, R. V. Characterization of surface acidity of an acid montmorillonite activated with hydrothermal, ultrasonic and microwave techniques. *Appl. Clay Sci.* **2006**, *31*, 16.
- (20) Mueller, R.; Kammler, H. K.; Wegner, K. OH surface density of SiO<sub>2</sub> and TiO<sub>2</sub> by thermogravimetric analysis. *Langmuir* **2003**, *19* (1), 160.
- (21) Vansant, E. F.; Van, D. V. P.; Vrancken, K. C. *Characterization and chemical modification of the silica surface*; Elsevier: Amsterdam, 1995.
- (22) Lin, Y. L.; Wang, T. J.; Jin, Y. Surface characteristics of hydrous silica coated TiO<sub>2</sub> particles. *Powder Technol.* **2002**, *123*, 196.

- (23) Cui, A. L. Studies on process, mechanism and new reactor of coating on surfaces of titania. Ph.D. Dissertation, Tsinghua University, Beijing, China, 1999.

*Received for review* July 27, 2006

*Revised manuscript received* November 29, 2006

*Accepted* December 2, 2006

IE060987Z